Parametrically excited hydrodynamic solitons

Guoqing Miao and Rongjue Wei
The State Key Laboratory of Modern Acoustics, The Institute of Acoustics, Nanjing University, Nanjing 210093, People's Republic of China
(Received 6 July 1998)

Based on the analysis of the recent experimental data, a new equation governing the motion of the solitons in a small rectangular water trough is proposed by using multiple-scale method. Both analytical and numerical analyses reveal that the equation gives a good explanation for some of the typical experimental observations on the evolution of the single and double solitons as well as the effect of surface tension on both breather and kink solitons. It also predicts the reflection of double-soliton at the end walls of the trough.
[S1063-651X(99)00804-1]

PACS number(s): 43.25.+y, 47.35.+i

The parametrically excited hydrodynamic soliton in a small water trough has been the one of the hot topics much discussed by many physicists and mathematicians. This study also provides an intuitive and vivid model for studying the general properties of the solitons in many other fields even beyond the scope of fluid dynamics in recent years. To date quite a few experimental results on parametrically excited solitons have been reported. Following the first observation of breather by Wu, Keolian, and Rudnik [1], the kink soliton has been found by Denardo, Wright, and Putterman [2]; the dynamic behavior of the solitons, for instance, the interaction between two as well as multiple solitons, the transition from period to chaos, has been studied by some authors [3–5]. The theoretical work was first carried out by Larraza and Putterman [6], Miles [7], and later by Guo-Xiang, Jia-ren, and Xian-Xi [8] and Xian-chu and Hongnong [9]. Taking into account driving, linear damping, and surface tension of the liquid, Miles arrived at a nonlinear Schrödinger equation modified to include the driving and linear damping [we refer to it as the modified nonlinear Schrödinger (MNLS) equation], which predicts analytically the existence of single breather and kink soliton, as well as the effect of surface tension on breather and kink solitons. To examine the effect of surface tension, in Ref. [10], the present authors have compared the distribution of both kinds of solitons on the phase plane of parameters kd vs σ ($\sigma \equiv \alpha k^2/\rho g$, α and ρ the surface tension coefficient and the density of the water, respectively, g the gravitational acceleration, $k=\pi/b$, b the width of the trough, d the depth of water), predicted from MNLS with the one measured experimentally, and found out an obvious discrepancy between the theory and the experiment: the theoretical distribution depends strongly on σ and kd, while the experimental one is independent of σ, but depends only on kd. We have thus made a qualitative explanation by comparing the potential energy of the free surface due to surface tension to that due to displacement. In this paper, analyzing and comparing the experimental data, and using multiple-scale method, a new equation governing the evolution of the solitons will be derived. Some characteristics of the equation will be discussed. A numerical analysis will be given to show the feasibility of the equation in explaining the experiments, and even to predict some new phenomena of the system.

Let the length of the trough be L. The velocity potential ϕ satisfies the following kinematic boundary value problem,

$$\nabla^2\phi=0, \quad -d\leqslant z\leqslant \eta, \tag{1}$$

$$\phi_x=0, \quad x=0,L, \tag{2}$$

$$\phi_y=0, \quad y=0,b, \tag{3}$$

$$\phi_z=0, \quad z=-d, \tag{4}$$

$$\phi_z=\eta_t+\phi_x\eta_x+\phi_y\eta_y, \quad z=\eta(x,y,t), \tag{5}$$

$$\phi_t+(g+\ddot{z}_0)\eta+\tfrac{1}{2}(\phi_x^2+\phi_y^2+\phi_z^2) = \frac{\alpha}{\rho}\frac{\eta_{xx}(1+\eta_y^2)+\eta_{yy}(1+\eta_x^2)-2\eta_x\eta_y\eta_{xy}}{(1+\eta_x^2+\eta_y^2)^{3/2}},$$

$$z=\eta(x,y,t), \tag{6}$$

where $\ddot{z}_0=-4\omega_0^2a_0\cos 2\omega_0 t$ is the driving acceleration exerted vertically on the trough, ω_0 approximates the natural frequency of the mode described by $k=\pi/b$ [called mode (0,1)], $\omega=(gkT)^{1/2}$ ($T\equiv\tanh kd$), of the trough, η is the free-surface displacement of water. For the typical experimental parameters $b=2.54$ cm, $d=2$ cm, $g=980$ cm/s^2, the corresponding value of ω is 34.6 rad/s, and $\omega_0=32.7$ rad/s, $a_0=0.07$ cm, $\alpha=70$ dyne/cm, $\rho=1$ g/cm^3, we have $4\omega_0^2a_0/g=0.31$ and $\sigma=0.11$. This shows that both $4\omega_0^2a_0/g$ and σ are of the same order of magnitude. We assume

$$4\omega_0^2a_0/g=0(\epsilon), \quad \sigma=0(\epsilon), \quad \beta\equiv\frac{\omega_0-\omega}{\epsilon\omega}=0(1), \tag{7}$$

with ϵ a small scale parameter. In Miles' theory σ was $0(1)$. Expand the boundary condition equations (5) and (6) to third order in η at $z=0$. According to the experiment, we consider that only the cross wave (in width direction of the trough), or the mode (0,1) was excited. and the soliton is the amplitude modulation of this mode in length direction. Introduce multiple-scale variable

$$x_j=\epsilon^j x, \quad t_j=\epsilon^j t, \quad (j=1,2,3,\ldots). \tag{8}$$

Expand ϕ and η as

$$\phi=\sum_{n=1}\epsilon^n\phi_n, \quad \eta=\sum_{n=1}\epsilon^n\eta_n. \tag{9}$$

Inserting Eqs. (8) and (9) into Eqs. (1) through (6), we will obtain a series of linear boundary value problems. Solving these problems successively, we will obtain the solutions of various order in ϵ. The first-order solution is

$$\phi_1=\frac{\cosh k(z+d)}{\cosh kd}[\psi(Z+Y)+\text{c.c.}], \tag{10}$$

$$\eta_1=\frac{i\omega}{g}[\psi(Z+Y)-\text{c.c.}], \tag{11}$$

where

$$Z=e^{i(ky-\omega t)}, \quad Y=e^{-i(ky+\omega t)}, \tag{12}$$

where c.c. is complex conjugate, ψ is a function of $x_1,x_2,t_1,t_2,\ldots$. To the second-order problem, the condition for eliminating the secular term for the first harmonic is

$$2i\psi_{t_1}+(2i\omega_0\gamma\sin 2\omega_0 t-\omega\gamma\cos 2\omega_0 t-\sigma\omega)\psi=0. \tag{13}$$

The second-order solution is

$$\phi_2=\frac{\cosh 2k(z+d)}{\cosh 2kd}\left[\frac{3k^2i(1+T^2)(1-T^2)}{4\omega T^2}\times\psi^2(Z^2+Y^2)+\text{c.c.}\right]+\left[\frac{-k^2i}{2\omega}(1+3T^2)\psi^2ZY+\text{c.c.}\right], \tag{14}$$

$$\eta_2=\frac{k^2(T^2-3)}{2gT^2}[\psi^2(Z^2+Y^2)+\text{c.c.}]+\frac{k^2(T^2+1)}{g}|\psi|^2[ZY^*+\text{c.c.}]+\frac{2k^2(T^2-1)}{g}|\psi|^2. \tag{15}$$

To the third-order problem, we will give only the compatible condition for the first harmonic, we have

$$i\left(\psi_{t_1}-\frac{\omega}{\omega_1}\gamma\psi^*_{t_1}+\delta\psi\right)+B\psi_{x_1x_1}+(\beta+A|\psi|^2)\psi+\gamma\psi^*=0, \tag{16}$$

where

$$\gamma=\frac{\omega_1\omega_0^2a_0(\omega+2\omega_0)}{\epsilon g\omega^2(2/\epsilon+\sigma/2)}, \quad B=\frac{1}{2/\epsilon+\sigma/2}, \tag{17}$$

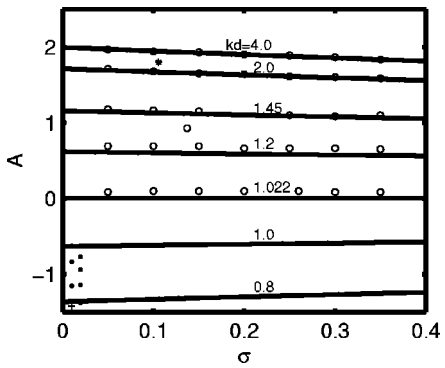

FIG. 1. A vs σ with kd as parameter. Also plotted are the experimentally measured distribution of breather and kink solitons. ○, breather; ●, kink; *. Wu's breather; +, Denardo's kink (the experimental data were taken from Refs. [1,2] and [10]).

$$A=\frac{6T^4-5T^2+16-9T^{-2}}{2(2/\epsilon+\sigma/2)}, \tag{18}$$

In Eq. (16) we have introduced linear damping by replacing $i(\partial/\partial t_1)$ with $i[(\partial/\partial t_1)+\delta]$, in which δ is the ratio of actual to critical damping for free oscillations. Equation (16) is just the evolution equation for the amplitude of the first-order solution. Compared to MNLS, a new term relative to driving, $-(\omega/\omega_1)\gamma\psi^*_{t_1}$, appears in Eq. (16). As MNLS does, Eq. (16) has steady ($\psi_{t_1}=0$, $\psi^*_{t_1}=0$) breather soliton solution for $kd>1.022$ ($A>0$),

$$\psi=M_1e^{i\theta}\,\text{sech}\left[M_1\left(\frac{A}{2B}\right)^{1/2}x_1\right], \tag{19}$$

and kink soliton solution for $kd<1.022$ ($A<0$),

$$\psi=M_2e^{i\theta}\tanh\left[M_2\left(\frac{|A|}{2B}\right)^{1/2}x_1\right], \tag{20}$$

with

$$\theta=\frac{\pi}{2}-\frac{1}{2}\sin^{-1}\frac{\delta}{\gamma}, \tag{21}$$

$$\tfrac{1}{2}AM_1^2+\beta-(\gamma^2-\delta^2)^{1/2}=0, \tag{22}$$

$$M_2^2|A|+\beta-(\gamma^2-\delta^2)^{1/2}=0. \tag{23}$$

One can see from Eq. (18) that due to $\sigma>0$, hence, the larger the σ, the smaller the magnitude of A, but σ does not influence the sign of A, which vanishes at $kd=1.022$. A vs σ with kd as parameter is plotted in Fig. 1, in which $A>0$ corresponds to $kd>1.022$, while $A<0$ corresponds to $kd<1.022$. Also plotted in Fig. 1 are the experimental results of ours [10], Wu [1], and Denardo [2]. One can see a good agreement between theory and experiments. At this point, we can say that the reason for the discrepancy between Miles' theory and experiment is the stronger effect of surface tension on the soliton being taken in the theory.

The stability analysis by Laedke *et al.* [11] is also applicable to the Eq. (16) for the stationary soliton solution. The condition

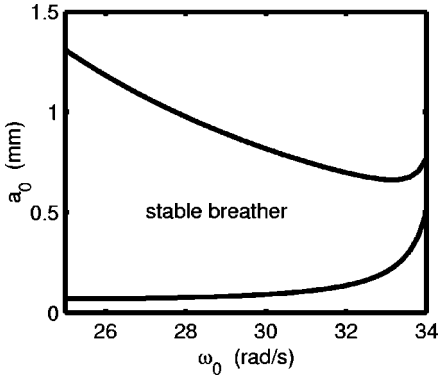

FIG. 2. The stability region for one breather soliton. $\omega=34.6$ rad/s, $\sigma=0.1$.

$$\delta^2<\gamma^2<\delta^2+\beta^2 \tag{24}$$

corresponds to the upper and lower limits of the driving amplitude, while the condition

$$\beta<0, \tag{25}$$

means $\omega_0<\omega$, corresponds to upper limit of the driving frequency. Figure 2 is a stability diagram for single breather soliton on a_0 vs ω_0 plane according to Eqs. (24) and (25) with typical experimental parameters. We see from Eq. (17) that as σ and/or δ are increased, the stability region moves up. This shows that the larger the σ and δ are, the larger the driving amplitude is needed to compensate the effects of the surface tension and the damping. The stability region measured experimentally is a limited region with some lower limit of driving frequency on a_0 vs the ω_0 plane [1]. The reason for this is that the soliton is the modulation of (0,1) mode, which becomes unstable below some driving frequency.

Next we investigate whether Eq. (16) can describe the complex dynamical behavior of the solitons found in the experiment, and even give us more information of the system. Owing to the nonintegrability of the Eq. (16), we have solved Eq. (16) numerically by using the implicit finite-difference algorithm. To check the effectiveness of the method, a numerical scheme was tested against the known standing soliton solution of Eq. (16) (with $\gamma=\delta=0$),

$$\psi=e^{i(\beta+A/2)t_1}\,\mathrm{sech}\left[\left(\frac{A}{2B}\right)^{1/2}x_1\right], \tag{26}$$

the computed results were found to deviated by less than 2–3 % from Eq. (26) after several periods passed for time t_1. Then we change driving amplitude and frequency and damping, and take single and double soliton as initial conditions and the boundary condition $(\partial\psi/\partial x_1)|_{x_1=0,\epsilon L}=0$. The typical results are indicated in Fig. 3. For the case of single soliton, when driving amplitude a_0 satisfies 0.065 cm $<a_0<0.075$ cm, the soliton is stable without any deformation for a long period. As a_0 is increased, say, $a_0=0.08$ cm, the wave form varies slightly with time [as seen in Fig. 3(a)]. When a_0 is increased further, the soliton becomes unstable, and destroyed due to the excitation of Stokes wave or other complex wave patterns. For the case of double solitons, an important result is the phenomenon of Farmi-Pasta-Ulam (FPU) recurrence. two solitons form a bound state, vibrate back and forth with each other [as shown in Fig. 3(b)]. These are in good agreement with experiments. As driving amplitude is increased, the calculated recurrence period and separation of two solitons increase, at last, they reflected at the boundary [Fig. 3(c)]. However, this has not yet been observed experimentally up to now. This is probably due to the strong friction between the liquid and the walls of the container. If one can diminish friction further between the liquid and the walls of the container, may be one can see the phenomenon predicted from above.

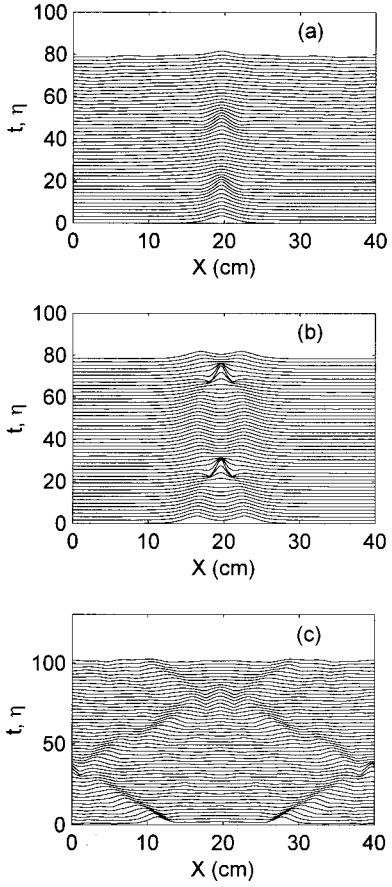

FIG. 3. The numerical results of Eq. (16). (a) One breather soliton with a slight change in wave form. $a_0=0.08$ cm. (b) FPU recurrence of double solitons; the recurrence period is 8 sec. $a_0=0.09$ cm. (c) The reflection of double soliton at the end walls of the trough. $a_0=0.11$ cm. $\omega_0=32.8$ rad/s for all cases.

In summary, based on the analysis of the experimental data, we have obtained a new equation (16) governing the motion of the solitons by using multiple-scale method. The analytical and numerical analysis reveal that the equation gives a good explanation for experimental observation on the evolution of single and double solitons, as well as the effect of surface tension on both breather and kink solitons. It also predicts the reflection of the double soliton at the end walls of the trough.

We are grateful to Professor Wei-zhong Chen for helpful discussions. This work was supported by The Chinese Nonlinear Science Foundation and The Chinese National Natural Science Foundation.

[1] Junru Wu, Robert Keolian, and Isadore Rudnick, Phys. Rev. Lett. **52**, 1421 (1984).
[2] Bruce Denardo, William Wright, and Seth Putterman, Phys. Rev. Lett. **64**, 1518 (1990).
[3] Xinlong Wang and Rongjue Wei, Phys. Rev. Lett. **78**, 2744 (1997).
[4] Xuenong Chen and Rongjue Wei, J. Fluid Mech. **259**, 291 (1994).
[5] Chen Weizhong, Wei Rongjue, and Wang Benren, Phys. Rev. E **53**, 6016 (1996).
[6] A. Larraza and S. Putterman, J. Fluid Mech. **148**, 443 (1984).
[7] John W. Miles, J. Fluid Mech. **148**, 451 (1984); **154**, 535 (1985).
[8] Huang Guo-xiang, Yan Jia-ren, and Dai Xian-xi, Acta Phys. Sin. **39**, 1234 (1990).
[9] Zhou Xian-chu and Cui Hong-nong, Sci. Sinica A **12**, 1269 (1992).
[10] Guoqing Miao and Rongjue Wei, Phys. Lett. A **220**, 87 (1996).
[11] E. W. Laedke and K. H. Spatschek, J. Fluid Mech. **223**, 589 (1991).